

Kinetic energy and fragment mass distributions for $^{240}\text{Pu}(\text{s.f.})$, $^{239}\text{Pu}(n_{\text{th}},f)$, and $^{240}\text{Pu}(\gamma,f)$

H. Thierens, A. De Clercq, E. Jacobs, D. De Frenne, P. D'hondt, P. De Gelder, and A. J. Deruytter
Nuclear Physics Laboratory, Proeftuinstraat 86, B-9000 Gent, Belgium

(Received 18 September 1980)

Energy correlation measurements were performed for $^{240}\text{Pu}(\text{s.f.})$, $^{239}\text{Pu}(n_{\text{th}},f)$, and the photofission of ^{240}Pu with 12-, 15-, 20-, and 30-MeV bremsstrahlung. The photofission cross section for ^{240}Pu was determined up to 30 MeV, which permitted the calculation of the average excitation energy $\langle E_{\text{exc}} \rangle$ of the compound nucleus. The average total kinetic energy $\langle E_k \rangle$ of the fragments for $^{240}\text{Pu}(\text{s.f.})$ was found to be 1.2 ± 0.5 MeV higher than for $^{239}\text{Pu}(n_{\text{th}},f)$. A decrease of $\langle E_k \rangle$, with $\langle E_{\text{exc}} \rangle$, $d\langle E_k \rangle/d\langle E_{\text{exc}} \rangle = -0.37 \pm 0.08$, is observed in the photofission of ^{240}Pu . Fragment shell effects are present in the kinetic energy and mass distributions for $^{240}\text{Pu}(\text{s.f.})$. Changes in the measured distributions with increasing excitation energy of the compound nucleus ^{240}Pu are discussed in the framework of the scission point model of Wilkins *et al.*

PACS numbers: 25.85. - w, 24.75. + i

<p>RADIOACTIVITY Fission $^{240}\text{Pu}(\text{s.f.})$. NUCLEAR REACTIONS Fission $^{239}\text{Pu}(n_{\text{th}},f)$, $^{240}\text{Pu}(\gamma,f)$, $E_{\gamma\text{max}}=12, 15, 20, 30$ MeV; measured: photofission yields, fragment energies E_1, E_2; deduced: $\sigma(\gamma,f)$, $N(\mu, E_k)/\langle E_{\text{exc}}(E_e) \rangle$.</p>

I. INTRODUCTION

A study of the excitation energy dependence of the total kinetic energy of the fragments for various mass splits yields information on the decrease of the influence of fragment shell effects and the coupling of fission to the other degrees of freedom. For the compound system ^{240}Pu , data on the kinetic energy release are available for the spontaneous fission from the ground state^{1,2} and from the isomeric state at 2.4 MeV (Ref. 3) and for fission induced in following reactions: $^{239}\text{Pu}(n,f)$,⁴ $^{239}\text{Pu}(d,pf)$,⁵ $^{240}\text{Pu}(\alpha, \alpha'f)$,³² and $^{241}\text{Pu}(^3\text{He}, \alpha f)$.⁶

Combining the total fragment kinetic energy results for spontaneous fission^{2,3} with those measured in the resonance around 4.65 MeV observed in the $^{239}\text{Pu}(d,pf)$ reaction, Lachkar *et al.*⁵ found experimental evidence for the existence of a superfluid mode below the fission barrier, as was proposed by Swiatecki and Bjørnholm.⁷ In this excitation energy range, the excitation energy of the fissioning nucleus would be converted almost entirely into additional pre-scission kinetic energy of the fragments for all mass splits. Above the fission barrier the average fragment kinetic energy $\langle E_k \rangle$ decreases with increasing excitation energy E_{exc} of the compound nucleus, the slope $d\langle E_k \rangle/dE_{\text{exc}}$ depends strongly on the used reaction. Generally, the observed decrease of $\langle E_k \rangle$ is found to be caused essentially by a decrease of the kinetic energies of the fragments for mass splits with heavy fragments in the mass region 125–140, due to the diminution of the influence of shell effects. Recently, from a study of the $^{241}\text{Pu}(^3\text{He}, \alpha f)$ reaction, Back *et al.*⁶ concluded that at near bar-

rier energies the primary reaction mechanism plays a decisive role and that the angular momentum transfer is not the determining parameter.

Concerning the fission parameters for the photofission of ^{240}Pu , no information is available in the literature. We performed energy correlation measurements for the photofission of ^{240}Pu with 12-, 15-, 20-, and 30-MeV bremsstrahlung. As the photon absorption (in our experiments) is mainly $E1$, predominantly 1^- states are excited in the ^{240}Pu nucleus. So in this work the fission of the compound system ^{240}Pu from essentially 1^- states is studied for average excitation energies varying from 9.4 to 13.3 MeV. In order to be able to determine these average excitation energies, a yield curve was measured for ^{240}Pu and the photofission cross section was determined from it up to 30 MeV, using the photon difference method described in Ref. 8. In addition we measured $^{240}\text{Pu}(\text{s.f.})$ and $^{239}\text{Pu}(n_{\text{th}},f)$. In $^{240}\text{Pu}(\text{s.f.})$ strong shell effects are present in the measured distributions. They decrease at higher excitation energies of the ^{240}Pu compound system. The results are explained in terms of the scission point model of Wilkins *et al.*⁹ In agreement with the conclusions of Nifenecker *et al.*¹⁰ the kinetic energy data are consistent with a weak coupling of the fission degree of freedom to quasiparticle excitations and a strong coupling to other, probably collective, modes.

II. EXPERIMENTAL PROCEDURE

The ^{240}Pu target consisted of a $109 \mu\text{g}/\text{cm}^2$ PuF_3 layer on a $40 \mu\text{g}/\text{cm}^2$ polyimide backing with $10 \mu\text{g}/\text{cm}^2$ gold. The isotopic composition of the plutonium was 0.68% ^{239}Pu , 98.47% ^{240}Pu , 0.48%

^{241}Pu , and 0.37% ^{242}Pu . For this target the contamination of the spontaneous fission data of ^{240}Pu with ^{242}Pu (s.f.) data was 0.7%. The ^{239}Pu target, used for the calibration, consisted of a 118 $\mu\text{g}/\text{cm}^2$ PuF_3 layer on an identical backing as the ^{240}Pu target; it was enriched up to 99.98% ^{239}Pu . The uncertainties on the thickness of the targets were of the order of 2%. The diameter of the active layer was 25 mm in both cases. The targets were prepared by the evaporation technique in the Central Bureau for Nuclear Measurements, Euratom, Geel.

The bremsstrahlung beam, produced in a 0.1 mm thick gold foil by an analyzed electron beam of the linac, was cleared of electrons by a cleaning magnet and collimated. The beam diameter at the target position was 15 mm. For the cross section measurements the photon beam intensity was measured with a replica of the NBS-P2 quantummeter¹¹ placed behind the fission chamber.

In the energy correlation measurements two Ortec F-series heavy ion detectors (CF-090-600-60) were mounted symmetrically on both sides of the fission target at an angle of 90° and at a distance of 7 cm from the beam axis. In this geometry 50 spontaneous fission events per day were observed. After amplification and shaping, the pulse heights of coincident ($\tau = 2 \mu\text{s}$) events were recorded by pairs in a 4096×4096 channels configuration using a PDP11 system with a Digital Equipment Corporation CA11C CAMAC interface and Northern Scientific NS 623 analog-to-digital converters. During the photofission runs a time gate of 5 μs , embracing the linac pulse, was set and an on-line correction of the fission fragment pulses for pileup during the linac pulses (γ flash) was performed as described in a previous paper.¹² By adjusting the electron current of the linac the γ flash was limited to 1% of the pulse height of the fission fragments. The spontaneous fission of ^{240}Pu was measured with the linac shut down.

Each experimental run at a given bremsstrahlung end-point energy or a spontaneous fission measurement was accompanied by a calibration run with 20-MeV bremsstrahlung. The stability of the measuring system was followed continuously with a precision pulser. At the end of the spontaneous fission and photofission measurements the ^{240}Pu photofission runs with 20-MeV bremsstrahlung were calibrated with $^{239}\text{Pu}(n_{\text{th}},f)$ using the Schmitt *et al.*¹³ calibration procedure and the parameters of Neiler *et al.*¹⁴ These calibrations were performed with a well-thermalized and collimated neutron beam of the reactor BR1 of the SCK/CEN Mol, Belgium. The same experimental setup and geometry as for the ^{240}Pu photofission measurements was used, while the stabil-

ity of the system was checked with a precision pulser and a ^{252}Cf (s.f.) source. Off line, the data were sorted in two-dimensional provisional mass μ and total kinetic energy E_k arrays, $N(\mu, E_k)$, of 120×120 channels.

For the determination of the photofission cross section of ^{240}Pu , a yield curve was measured with four heavy ion detectors mounted in a plane in front of the target. The yield curve, deduced from the pulse height spectra obtained in the four detectors, was measured for bremsstrahlung end-point energies between 10 and 32 MeV. The measuring bin width was 500 keV for bremsstrahlung end-point energies between 10 and 20 MeV and 1 MeV for bremsstrahlung end-point energies between 20 and 32 MeV. For the behavior of the yield curve from the threshold up to 7.5 MeV the cross section data of Rabotnov *et al.*¹⁵ were used. In the remaining energy region, from 8 up to 9.5 MeV, an interpolation between the data of Rabotnov *et al.*¹⁵ and our data was performed. For the derivation of the cross section, the method of Crawford *et al.*,⁸ containing a decorrelation of errors of photon difference data, was used. The analysis bin width was 2 MeV. To obtain the absolute values of the cross section, normalization relative to the photofission of ^{235}U with 12- and 18-MeV end-point bremsstrahlung was performed using the cross section data of Caldwell *et al.*¹⁶ For this purpose the ^{240}Pu target was replaced by a ^{235}U target with the same dimensions.

III. RESULTS AND DISCUSSION

A. Photofission cross section and average excitation energies

The cross section for the photofission of ^{240}Pu up to 30 MeV obtained from our experiments is presented in Fig. 1. Up to 7.5 MeV the cross section was adopted from Rabotnov *et al.*,¹⁵ as already mentioned. The error bars in the figure include

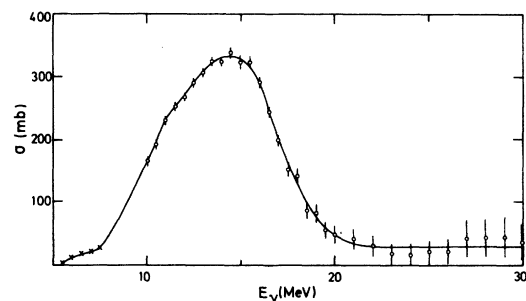


FIG. 1. Photofission cross section of ^{240}Pu , including second and multiple chance fission.

only the statistical uncertainties on the measured yields. For an estimation of the absolute uncertainties on the cross section values a systematic contribution of 10%, due to the uncertainties on the target thicknesses and the reproducibility of the target detectors and beam geometry, has to be included.

The photofission cross section shows the typical giant resonance structure as generally observed for actinide nuclei. It has a maximum value of 340 mb at 14.5 MeV and a full width at half maximum of 7.3 MeV. The integrated cross section up to 20 MeV is 2.6 ± 0.1 MeV b. Above 20 MeV, up to 30 MeV, the obtained cross section is low and almost constant (30 mb). Such a behavior was also found by Katz *et al.*¹⁷ for the cross section for asymmetric fission in the photofission of ^{238}U .

For fission induced by 12 MeV bremsstrahlung a value of 0.68 ± 0.06 was found for the ^{235}U to ^{240}Pu fission yield. The study of the photoneutron and photofission cross sections for ^{235}U , ^{236}U , ^{238}U , and ^{232}Th of Caldwell *et al.*¹⁶ shows that the total photon-absorption cross sections are roughly the same and that the neutron-to-fission branching ratio Γ_n/Γ_f remains almost constant above 9 MeV. Based on these observations and adopting $\Gamma_n/\Gamma_f = 1.4$ for ^{235}U (see Ref. 16), the value $\Gamma_n/\Gamma_f = 0.63 \pm 0.15$ is deduced for ^{240}Pu from our measured ^{235}U to ^{240}Pu photofission yield ratio. The Γ_n/Γ_f values determined by Caldwell *et al.*¹⁶ show an exponential decrease with the fissility parameter Z^2/A . Extrapolation of this behavior to the plutonium region yields $\Gamma_n/\Gamma_f = 0.25$ for ^{240}Pu . The value of 0.63 obtained from our results is higher than this expected ratio. However, the Γ_n/Γ_f values in this Z^2/A region, determined in other experiments, are also, in agreement with our result, higher than expected from the dependence deduced by Caldwell *et al.* (see Ref. 16). Our result also agrees very well with the exponential dependence of Γ_n/Γ_f versus mass number, deduced by Vandenbosch and Huizenga.¹⁸ Following these authors one would expect $\Gamma_n/\Gamma_f = 0.60$ for ^{240}Pu .

Starting from the deduced cross section, the average excitation energy of the compound nucleus ^{240}Pu , $\langle E_{\text{exc}}(E_e) \rangle$, corresponding to the different end-point energies of the bremsstrahlung, was calculated in the same way as in a previous paper.¹⁹ Average excitation energy values of 9.4, 11.1, 12.6, and 13.3 MeV, respectively, were obtained for bremsstrahlung end-point energies of 12, 15, 20, and 30 MeV.

Because the separate cross sections $\sigma(\gamma, f)$ and $\sigma(\gamma, nf)$ are not determined for ^{240}Pu , the contribution of second chance fission in our ^{240}Pu experiments cannot be calculated. From the measured photofission cross section of ^{240}Pu and adopting,

for the photofission of ^{240}Pu , the first chance to total photofission cross section ratio of ^{235}U , determined by Caldwell *et al.*,¹⁶ the second chance fission contribution in our experiments with 12-, 15-, and 20-MeV bremsstrahlung would be 0%, 8%, and 20%, respectively. In view of the dependence of Γ_n/Γ_f on Z^2/A , the second chance fission contributions in our photofission experiments on ^{240}Pu are less than these estimated values.

B. Kinetic energy

In Fig. 2 the obtained overall total kinetic energy distributions for $^{240}\text{Pu}(s.f.)$ and $^{239}\text{Pu}(n_{\text{th}}, f)$ are compared. In the case of $^{240}\text{Pu}(s.f.)$ the distribution is asymmetric and shows a significant deviation from a Gaussian shape. This deviation was already observed by Toraskar and Melkonian¹ and Deruytter and Wegener-Penning,² but a possible

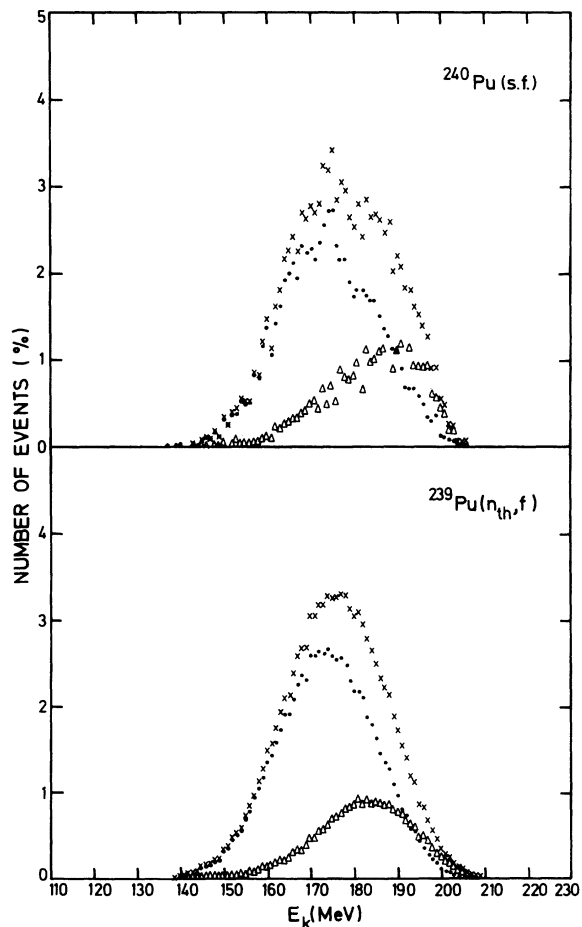


FIG. 2. Overall total kinetic energy distributions for $^{240}\text{Pu}(s.f.)$ and $^{239}\text{Pu}(n_{\text{th}}, f)$ represented by crosses. The total kinetic energy distributions for fragments with heavy mass inside and outside the mass interval 130–135 are indicated by triangles and dots, respectively.

explanation for this effect was not indicated by these authors. In the work of Toraskar and Melkonian the possibility that this structure was caused by a $^{252}\text{Cf}(\text{s.f.})$ contamination was excluded.

A decomposition of the overall total kinetic energy distribution shows that the total kinetic energy distribution for the mass splits in the heavy mass region 130–135 is asymmetric and is strongly different for $^{240}\text{Pu}(\text{s.f.})$ ($\langle E_k \rangle_{130-135} = 184.16$ MeV, dissymmetry coefficient $\mu_3/\sigma^3 = -0.69$) and for $^{239}\text{Pu}(n_{\text{th}},f)$ ($\langle E_k \rangle_{130-135} = 181.90$ MeV, $\mu_3/\sigma^3 = -0.41$), while the total kinetic energy distribution for the other mass splits ($m_H < 130$ and $m_H > 135$), having a nearly Gaussian shape, remains practically unchanged in the two cases. This decomposition shows that for $^{240}\text{Pu}(\text{s.f.})$ the observed important deviation of the overall total kinetic energy distribution from the Gaussian shape is predominantly due to the strongly dissymmetric total kinetic energy distribution for mass splits with heavy mass in the region 130–135. The observed dissymmetry can be understood in the scission point model of Wilkins *et al.*⁹ by the preferential formation of a shell-stabilized configuration with small deformation ($\beta_1 + \beta_2 \sim 0.95$) for mass splits with the heavy fragments in the region around the $N = 82$ closed neutron shell, compared to a second stabilized scission configuration in the same mass region, having a larger deformation ($\beta_1 + \beta_2 \sim 1.4$), which is favored by a liquid drop behavior. The disappearance of the shoulder in the overall kinetic energy distribution in $^{239}\text{Pu}(n_{\text{th}},f)$ can be explained by a decrease of the shell corrections at higher intrinsic temperatures.

Some important quantities of the overall kinetic

energy and mass distributions are summarized in Table I. The average value of the measured post- and pre-neutron total kinetic energy of the fragments and its standard deviation are indicated by $\langle E_k \rangle$, $\langle E_k^* \rangle$, and σ_{E_k} . The number of measured fission events is indicated by NEV. In addition the average mass of the light and heavy fragment peaks of the overall provisional and pre-neutron mass distributions are given in this table. They are denoted by $\langle \mu_L \rangle$, $\langle \mu_H \rangle$ and $\langle m_L^* \rangle$, $\langle m_H^* \rangle$; the corresponding standard deviations are denoted by $\sigma(\mu_L)$ and $\sigma(\mu_H)$. The uncertainties on the values given in the table are the root-mean-square deviations for at least seven experimental runs. The values for the peak-to-valley ratios of the provisional mass distributions P/V together with their statistical uncertainties are also given in Table I. For the calculation of the average total pre-neutron kinetic energies $\langle E_k^* \rangle$ from the corresponding $\langle E_k \rangle$ values we used the measured values 2.15 ± 0.06 (Ref. 20) and 2.892 ± 0.027 (Ref. 18) of the average number of emitted neutrons, $\langle \nu_T \rangle$, for $^{240}\text{Pu}(\text{s.f.})$ and $^{239}\text{Pu}(n_{\text{th}},f)$, respectively. In photofission of ^{240}Pu , however, no information on the dependence of the neutron emission on the excitation energy is available. For the neutron emission correction of the photofission $\langle E_k \rangle$ values, the linear dependence of $\langle \nu_T \rangle$ on the excitation energy, with a slope 0.134 n/MeV, found in fast neutron induced fission,²¹ was adopted. In comparing the kinetic energy results for the photofission and the spontaneous fission of ^{240}Pu with $^{239}\text{Pu}(n_{\text{th}},f)$ an additional systematic error of 200 keV, due to the uncertainties in the thickness of the targets has to be added to the errors given in the table.

TABLE I. Parameters of the overall kinetic energy and mass distributions for $^{240}\text{Pu}(\text{s.f.})$, $^{239}\text{Pu}(n_{\text{th}},f)$, and the photofission of ^{240}Pu .

	$^{240}\text{Pu}(\text{s.f.})$	$^{239}\text{Pu}(n_{\text{th}},f)$	$^{240}\text{Pu}(\gamma,f)$			
			$E_e = 12$ MeV	$E_e = 15$ MeV	$E_e = 20$ MeV	$E_e = 30$ MeV
NEV	7262	101×10^3	12×10^3	51×10^3	355×10^3	113×10^3
$\langle E_k \rangle$ (MeV)	177.25 ± 0.30	175.57	173.99 ± 0.24	173.25 ± 0.24	172.46 ± 0.20	172.22 ± 0.31
$\langle E_k^* \rangle$ (MeV)	178.85 ± 0.30	177.69	176.39 ± 0.24	175.80 ± 0.24	175.15 ± 0.20	174.98 ± 0.31
σ_{E_k} (MeV)	11.99 ± 0.20	11.84	11.86 ± 0.14	11.94 ± 0.15	12.22 ± 0.12	12.37 ± 0.10
$\langle \mu_L \rangle$ (u)	101.53 ± 0.20	100.68	100.50 ± 0.14	100.48 ± 0.09	100.57 ± 0.08	100.72 ± 0.14
$\langle \mu_H \rangle$ (u)	138.47 ± 0.20	139.32	139.50 ± 0.14	139.52 ± 0.09	139.43 ± 0.08	139.28 ± 0.14
$\sigma_{\mu_L} = \sigma_{\mu_H}$ (u)	5.70 ± 0.12	6.69	7.16 ± 0.10	7.36 ± 0.08	7.64 ± 0.06	7.82 ± 0.08
$\langle m_L^* \rangle$ (u)	101.26 ± 0.20	100.33	100.12 ± 0.14	100.08 ± 0.09	100.16 ± 0.08	100.29 ± 0.14
$\langle m_H^* \rangle$ (u)	138.74 ± 0.20	139.67	139.88 ± 0.14	139.92 ± 0.09	139.84 ± 0.08	139.71 ± 0.14
P/V	400 ± 180	100 ± 9	27 ± 3	20.6 ± 1.3	13.1 ± 0.4	9.3 ± 0.3
E_{exc} (MeV)	0	6.5	9.4	11.1	12.6	13.3

The $\langle E_h^* \rangle$ value for $^{240}\text{Pu}(\text{s.f.})$ is 1.2 ± 0.5 MeV higher than for $^{239}\text{Pu}(n_{\text{th}},f)$. The difference was already determined by Toraskar and Melkonian,¹ by Deruytter and Wegener-Penning,² and recently by Wagemans *et al.*²² Toraskar and Melkonian reported 3.7 ± 3.0 MeV for the difference in $\langle E_h^* \rangle$ between $^{240}\text{Pu}(\text{s.f.})$ and $^{239}\text{Pu}(n_{\text{th}},f)$. Because they used different calibration targets during their experiments and because the $\langle E_h^* \rangle$ value for $^{239}\text{Pu}(n_{\text{th}},f)$ from their measurements, 175.2 MeV, is about 2.5 MeV too low, these $\langle E_h^* \rangle$ values are not reliable. Using a target with a mixed composition of ^{239}Pu and ^{240}Pu , Deruytter and Wegener-Penning² found for $^{240}\text{Pu}(\text{s.f.})$ an $\langle E_h^* \rangle$ value 1.1 ± 0.2 MeV lower than for $^{239}\text{Pu}(n_{\text{th}},f)$. The discrepancy between this and our result is difficult to explain. Possible reasons are perhaps the instability of the measuring system during the experiments of Deruytter and Wegener-Penning, leading to the use of time dependent calibration constants, or inhomogeneities in the electro-sprayed target, yielding a bad resolution.

Also for the fissioning system ^{242}Pu , $\langle E_h^* \rangle$ was found to be higher in spontaneous fission than in thermal neutron induced fission. Dyatchenko *et al.*²³ reported a value of 2.6 ± 0.3 MeV for the difference in $\langle E_h^* \rangle$. By comparing the measured $\langle \nu_T \rangle$ value of 2.16 ± 0.06 (Ref. 20) for $^{240}\text{Pu}(\text{s.f.})$ with an extrapolation to zero excitation energy of $\langle E_h^* \rangle$ and $\langle \nu_T \rangle$ for the compound nucleus ^{240}Pu , and using the dependence of $\langle E_h^* \rangle$ and $\langle \nu_T \rangle$ on the excitation energy deduced in fast neutron fission,^{4,21} an expectation value for the kinetic energy in the spontaneous fission can be obtained, based on energy balance considerations. Following Patin *et al.*²⁴ the extrapolated values for $\langle E_h^* \rangle$ and $\langle \nu_T \rangle$ at zero excitation energy are 180.3 MeV and 1.98. Because the average γ energy released per fission event is the same in $^{240}\text{Pu}(\text{s.f.})$ as in $^{239}\text{Pu}(n_{\text{th}},f)$ (Ref. 25) and adopting from Nifenecker *et al.*²⁶ that the energy needed to emit an additional neutron is about 8.6 MeV, the obtained expectation value for $\langle E_h^* \rangle$ in $^{240}\text{Pu}(\text{s.f.})$ is 178.8 MeV. Finally, after correction for the important differences in the mass distribution (see Sec. IIIC), by adopting the $\langle Q \rangle(m^*)$ values from Ref. 14 for the compound system ^{240}Pu and by using the mass distributions determined in this work, the expectation value for $\langle E_h^* \rangle$ in the spontaneous fission of ^{240}Pu is 179.4 MeV, in good agreement with our experimentally determined value.

In Fig. 3 the $\langle E_h^* \rangle$ values deduced from the $^{239}\text{Pu}(d,pf)$ reaction data by Lachkar *et al.*⁵ and from the $^{239}\text{Pu}(n,f)$ reaction data by Akimov *et al.*⁴ are compared with the $\langle E_h^* \rangle$ values of Weber *et al.*³ for isomeric fission and with the data obtained in this work. The $\langle E_h^* \rangle$ value, $179.5^{+1.5}_{-0.7}$ MeV, in the

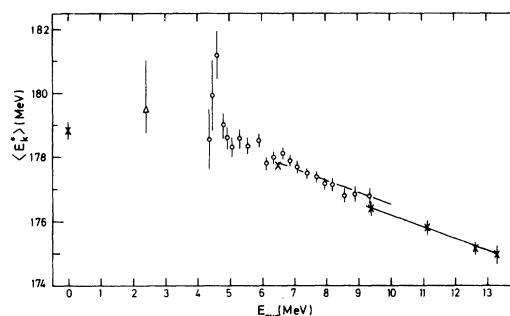


FIG. 3. $\langle E_h^* \rangle$ values as a function of the excitation energy of the compound nucleus ^{240}Pu . The values obtained by the $^{239}\text{Pu}(d,pf)$ reaction (Ref. 5) and by the $^{239}\text{Pu}(n,f)$ reaction (Ref. 4) are given in the figure together with our results and the value for the spontaneous fission from the isomeric state (Ref. 3). They are represented by open circles, a dashed line, crosses, and a triangle, respectively.

spontaneous fission from the isomeric state at 2.4 MeV lies very close to the spontaneous fission value from the ground state determined in this work. By combining the spontaneous fission data of Deruytter *et al.*² and the isomeric fission data of Weber *et al.*³ with the kinetic energy value in the "resonance" around 4.65 MeV, observed in their $^{239}\text{Pu}(d,pf)$ reaction work, Lachkar *et al.*⁵ concluded that in the fissioning system ^{240}Pu below the barrier the additional excitation energy is transformed totally into kinetic energy of the fragments, resulting in $d\langle E_h^* \rangle/dE_{\text{exc}} = +1$. This would indicate that the fission degree of freedom is very weakly coupled to other (collective or intrinsic) degrees of freedom in this excitation energy region (superfluid mode). Using our value for $\langle E_h^* \rangle$ in $^{240}\text{Pu}(\text{s.f.})$, the slope $d\langle E_h^* \rangle/dE_{\text{exc}}$, obtained by a least squares fit, is reduced to a value of $+0.47 \pm 0.18$. Thus, for the fissioning system ^{240}Pu below the fission barrier, the superfluid fission mode as proposed by Lachkar *et al.*⁵ does not exist. This is in agreement with the results obtained in other fissioning systems, where a strong coupling of the fission degree of freedom to other degrees of freedom (especially collective) is observed.¹⁰

The full line in Fig. 3, having a slope $d\langle E_h^* \rangle/d\langle E_{\text{exc}}(E_e) \rangle = -0.37 \pm 0.08$, represents a linear fit to our photofission data, using a weighted least squares procedure. For the excitation energy of the compound nucleus the average excitation energy $\langle E_{\text{exc}}(E_e) \rangle$, calculated in Sec. IIIA, was adopted. The fit to the results of Akimov *et al.*⁴ obtained by fast neutron induced fission of ^{239}Pu in the excitation energy region 6.6–10 MeV, is indicated in Fig. 3 by the dashed line. The value $d\langle E_h^* \rangle/dE_{\text{exc}} = -0.35 \pm 0.05$ is, within the uncer-

tainties, the same as obtained in our photofission experiments at higher excitation energies. Also in the $^{239}\text{Pu}(d, pf)$ reaction, Lachkar *et al.*²⁷ found for the slope $d\langle E_k^* \rangle / dE_{\text{exc}}$, in the excitation energy range 4.5–9.5 MeV, values which are in very good agreement with our photofission results. Not only the variation of the kinetic energy with excitation energy, but also the absolute value of the average total fragment kinetic energy for the photofission of ^{240}Pu with 12-MeV bremsstrahlung (corresponding to an average excitation energy of 9.4 MeV) agrees with the data from the $^{239}\text{Pu}(n, f)$ and $^{239}\text{Pu}(d, pf)$ reactions, taking into account the mentioned additional 200 keV contribution in the uncertainty on the $\langle E_k^* \rangle$ values. This similar behavior of $\langle E_k^* \rangle$ in photofission and neutron induced fission supports the adoption of the excitation energy dependence of $\langle \psi_T \rangle$ from $^{239}\text{Pu}(n, f)$ in our photofission studies for the determination of the pre-neutron kinetic energies from the measured ones.

In the $^{240}\text{Pu}(\alpha, \alpha'f)$ reaction, however, as reported by Back *et al.*,⁶ Wolf *et al.*³² observed a stronger decrease of $\langle E_k^* \rangle$ with increasing E_{exc} . They found $d\langle E_k^* \rangle / dE_{\text{exc}} = -1.1 \pm 0.1$. Back *et al.*⁶ found for the $^{241}\text{Pu}(^3\text{He}, \alpha f)$ reaction a change of this slope around 9 MeV: below 9 MeV, $d\langle E_k^* \rangle / dE_{\text{exc}} = -0.05 \pm 0.10$; in the energy region 9–13 MeV, $d\langle E_k^* \rangle / dE_{\text{exc}} = -0.65 \pm 0.04$. In the $^{240}\text{Pu}(\gamma, f)$, $^{239}\text{Pu}(n, f)$, and $^{239}\text{Pu}(d, pf)$ reactions, yielding about the same value for $d\langle E_k^* \rangle / dE_{\text{exc}}$, the angular momentum transfer to the compound system is small [$1 \sim 1\hbar$ in E1 absorption, $1 \sim 1-2\hbar$ in neutron capture, and $1 \sim 2-3\hbar$ in the (d, pf) reaction]. In the $^{240}\text{Pu}(\alpha, \alpha'f)$ and $^{241}\text{Pu}(^3\text{He}, \alpha f)$ reactions higher spin states ($6-7\hbar$) are populated. This would lead to the conclusion that the slope $d\langle E_k^* \rangle / dE_{\text{exc}}$ depends on the angular momentum transfer in the reaction. However, from the results of the study of the $^{240}\text{Pu}(\alpha, \alpha'f)$ and $^{241}\text{Pu}(^3\text{He}, \alpha f)$ reactions Back *et al.*⁶ concluded that not the angular momentum transfer, but the reaction mechanism is the decisive parameter, determining the dependence of the kinetic energy of the fragments on the excitation energy of the compound system.

For the interpretation of the changes in the average kinetic energy with the excitation energy, observed in our experiments, the dependence of the kinetic energy on the fragment mass and the excitation energy of the compound nucleus was studied. In Fig. 4 a comparison is made between the variation of the average pre-neutron kinetic energy with the heavy fragment mass for the spontaneous fission of ^{240}Pu , the thermal neutron induced fission of ^{239}Pu , and the photofission of ^{240}Pu with 20-MeV bremsstrahlung, corresponding to an average excitation energy of 12.6 MeV. For

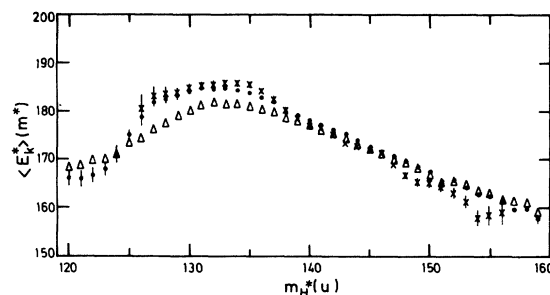


FIG. 4. Average pre-neutron kinetic energy $\langle E_k^* \rangle (m^*)$ as a function of the heavy fragment mass for $^{240}\text{Pu}(\text{s.f.})$, $^{239}\text{Pu}(n_{\text{th}}, f)$, and ^{240}Pu photofission with 20-MeV bremsstrahlung. The $^{240}\text{Pu}(\text{s.f.})$ results are represented by crosses, the $^{239}\text{Pu}(n_{\text{th}}, f)$ results by dots and the photofission result by triangles.

the calculation of these functions from the $N(\mu, E_k)$ arrays, the neutron emission curve $\nu(m^*)$ of Milton and Fraser²⁸ for $^{239}\text{Pu}(n_{\text{th}}, f)$ was used, multiplied with an appropriate ratio to obtain the correct average number of emitted neutrons. This procedure was necessary due to the lack of experimental information on the spontaneous fission and photofission of ^{240}Pu . The variation of the average measured kinetic energy as a function of the heavy provisional mass shows the same behavior as presented in Fig. 4. Except in the cases where the error bars are given in the figure, the uncertainties have the sizes of the points.

The differences between $^{240}\text{Pu}(\text{s.f.})$ and $^{239}\text{Pu}(n_{\text{th}}, f)$ are negligible except in the mass region 132–136, where the kinetic energy is higher for the spontaneous fission, and above heavy mass 146, where the kinetic energy is increased for $^{239}\text{Pu}(n_{\text{th}}, f)$. The decrease in $^{239}\text{Pu}(n_{\text{th}}, f)$ in the mass region around the closed $N = 82$ neutron shell can be explained in the scission point model of Wilkins *et al.*⁹ by a diminution of the shell corrections at higher intrinsic temperatures, leading to scission configurations with larger deformations, as mentioned in the beginning of this section. In the comparative studies of Unik *et al.*²⁹ of the fissioning systems $^{246}\text{Cm}(\text{s.f.})$, $^{245}\text{Cm}(n_{\text{th}}, f)$, $^{250}\text{Cf}(\text{s.f.})$, and $^{249}\text{Cf}(n_{\text{th}}, f)$ it also appears that the kinetic energy remains practically constant in the mass region 140–145, while at higher fragment mass the kinetic energy is higher in neutron induced fission. However, below heavy mass 140 the total fragment kinetic energy is also higher for the thermal neutron induced fission of ^{249}Cf than for $^{250}\text{Cf}(\text{s.f.})$. For the fissioning system ^{246}Cm the kinetic energy is only slightly higher in the thermal neutron induced fission in this mass region, so that ^{246}Cm takes an intermediary place between ^{240}Pu and ^{250}Cf . Although the intrinsic temperature depends on the compound nucleus and shell

corrections increase at low intrinsic temperatures,⁹ the observed behavior in the three cases is difficult to explain.

The differences between the behavior of $\langle E_h^* \rangle(m^*)$ for $^{239}\text{Pu}(n_{\text{th}},f)$ and the photofission of ^{240}Pu with 20 MeV bremsstrahlung in the mass region above the heavy mass 140 are completely negligible, as can be seen in Fig. 4. In the symmetric mass region the kinetic energy is slightly higher for photofission (a tendency also present in the provisional mass distributions). In the mass region around mass 130 a strong decrease of the kinetic energy in photofission compared to $^{239}\text{Pu}(n_{\text{th}},f)$ and $^{240}\text{Pu}(s.f.)$ is observed, that accounts almost totally for the decrease of the average total fragment kinetic energy.

A study of the variation of $\langle E_h^* \rangle(m^*)$ with the average excitation energy in the photofission of ^{240}Pu shows completely the same behavior as can be seen in Fig. 5, where the coefficient $d\langle E_h^* \rangle(m^*)/d\langle E_{\text{exc}}(E_e) \rangle$, obtained from our photofission results, is given. For strongly asymmetric mass splits, the region where shell effects are of minor importance, this coefficient practically vanishes, indicating that the fission degree of freedom is very weakly coupled to quasiparticle excitations. In the symmetric fission region the coefficient is slightly positive, although no definite conclusions can be drawn in view of the large experimental uncertainties. In the transitional re-

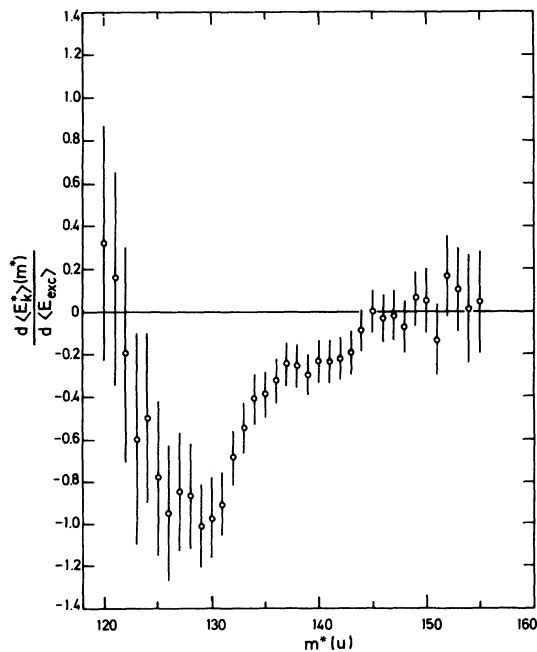


FIG. 5. Variation of $\langle E_h^* \rangle(m^*)$ with $\langle E_{\text{exc}}(E_e) \rangle$ for the photofission of ^{240}Pu .

gion from symmetric-to-asymmetric fission the slope $d\langle E_h^* \rangle(m^*)/d\langle E_{\text{exc}}(E_e) \rangle$ shows a strong dip with a minimum value of -1.0 around mass 129–130. The dependence of $\langle E_h \rangle(\mu)$ on the excitation energy has completely the same behavior as $\langle E_h^* \rangle(m^*)$, given in Fig. 5, indicating that the choice of the neutron emission curve does not seriously influence our results. The behavior of $d\langle E_h^* \rangle(m^*)/d\langle E_{\text{exc}}(E_e) \rangle$, deduced in this work for the photofission of ^{240}Pu is in very good agreement with the results obtained from fission induced by other reactions (see, e.g., Ref. 30). The variation of $\langle E_h^* \rangle(m^*)$ and $\langle E_h \rangle$ with $E_{\text{exc}}(E_e)$, observed in the photofission of ^{240}Pu , can be explained by the model of Wilkins *et al.*⁹ The changes in the kinetic energy can be attributed to the decrease, at higher intrinsic temperatures, of shell corrections, which are especially prominent in the mass region around mass 130. Around mass 130 a secondary configuration with larger deformation, competing with the shell-stabilized configuration, becomes of more importance at higher intrinsic temperatures.

The mass dependence of the width of the kinetic energy distribution $\sigma_{E_h}(\mu)$ for the studied fissioning systems is presented in Fig. 6. For $^{240}\text{Pu}(s.f.)$, $^{239}\text{Pu}(n_{\text{th}},f)$, and the photofission of ^{240}Pu with 12-MeV bremsstrahlung the $\sigma_{E_h}(\mu)$ values were averaged over three masses in the symmetric mass region, because of the poor statistics. The dashed line in the figure for $^{240}\text{Pu}(s.f.)$ represents the $\sigma_{E_h}(\mu)$ behavior for $^{240}\text{Pu}(n_{\text{th}},f)$, to compare the two fissioning systems. The differences are within the error bars although there is a tendency for an increase of the width for strongly asymmetric mass splits in the case of $^{239}\text{Pu}(n_{\text{th}},f)$.

To ease the comparison between the curves for $^{239}\text{Pu}(n_{\text{th}},f)$ and for the photofission of ^{240}Pu with bremsstrahlung with different end-point energies, the smooth curve drawn through the data points for 20-MeV bremsstrahlung is reproduced in the other cases, but shifted over a constant amount: -0.6 MeV in the case of $^{239}\text{Pu}(n_{\text{th}},f)$ and $^{240}\text{Pu}(\gamma_{12\text{MeV}},f)$, -0.4 MeV for $^{240}\text{Pu}(\gamma_{15\text{MeV}},f)$, and $+0.2$ MeV for $^{240}\text{Pu}(\gamma_{30\text{MeV}},f)$. Figure 6 shows that, except for the mass independent shift, the mass dependence of $\sigma_{E_h}(\mu)$ is the same for each bremsstrahlung end-point energy. The maxima of $\sigma_{E_h}(\mu)$ in photofission are reached in the mass region 126–127. The differences of $^{239}\text{Pu}(n_{\text{th}},f)$ with photofission are also small for mass splits with the heavy fragment in the mass region above mass 135. From the work of Asghar *et al.*,³¹ who performed a detailed study of $^{239}\text{Pu}(n_{\text{th}},f)$ with sufficient statistics (3.6×10^6 counts), follows that $\sigma_{E_h}(\mu)$ reaches a sharp maximum of 12.4 MeV for mass 123. The maximum present at mass

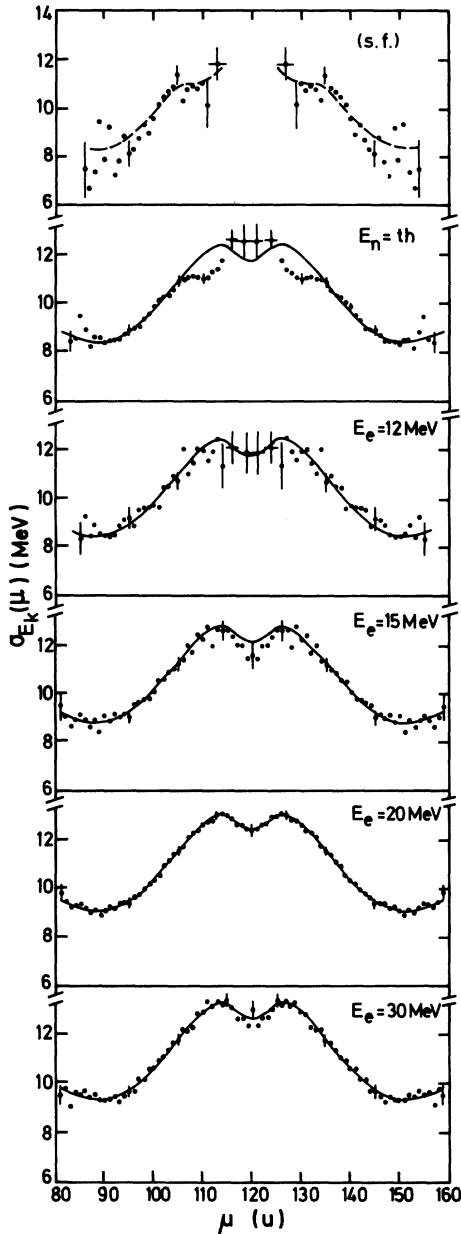


FIG. 6. Variance $\sigma_{E_k}(\mu)$ of the total kinetic energy distributions, as a function of the provisional fragment mass for $^{240}\text{Pu}(\text{s.f.})$, $^{239}\text{Pu}(n_{\text{th}},f)$, and the photofission of ^{240}Pu . The end-point energy of the bremsstrahlung is indicated by E_e .

123 for low excitation energy of the compound system, originates in the framework of the model of Wilkins *et al.*⁹ from a competition between comparable shell corrections for neutron numbers around $N=75$, resulting in different possible stable scission configurations with different deformations and thus resulting in a broad distribution of the distances between the charge centers of the fragments at the moment of scission. The

increase of the width of the $E_k(\mu)$ distribution for the photofission of ^{240}Pu compared to $^{239}\text{Pu}(n_{\text{th}},f)$ in the mass region around mass 130 can be understood in the same way as the dip in the $d\langle E_k^* \rangle(m^*)/d\langle E_{\text{exc}} \rangle$ behavior. Due to the diminution of shell effects at higher excitation energies the distribution of the distances between the charge centers is broadened by the enhanced production of a secondary scission configuration with a total deformation $\beta_1 + \beta_2 \sim 1.40$, competing with the shell stabilized configuration with a total deformation $\beta_1 + \beta_2 \sim 0.95$.

C. Mass distribution

The parameters of the mass distributions for $^{240}\text{Pu}(\text{s.f.})$, $^{239}\text{Pu}(n_{\text{th}},f)$, and the photofission of ^{240}Pu with 12-, 15-, 20-, and 30-MeV bremsstrahlung are given in Table I. As generally observed, a decrease of P/V with increasing excitation energy of the compound nucleus is found. The P/V ratio, 150, obtained in radiochemical measurements for $^{239}\text{Pu}(n_{\text{th}},f)$ (see Ref. 18) is significantly higher than the value that we deduced for the provisional mass distributions. This is due to the mass resolution inherent in the method, the neutron emission, and the geometry in our experimental setup. The P/V values 100 ± 35 and 27 ± 4 obtained by Wagemans *et al.*²² for $^{240}\text{Pu}(\text{s.f.})$ and $^{239}\text{Pu}(n_{\text{th}},f)$, respectively, indicate a much poorer (mass) resolution in their experiments, compared to ours. For the photon induced fission of ^{240}Pu , a comparison with other authors is not possible, as no information on this subject is available.

The parameters $\langle \mu_L \rangle$ and $\langle \mu_H \rangle$ have almost the same value in photofission of ^{240}Pu as in $^{239}\text{Pu}(n_{\text{th}},f)$, and remain practically constant for different end-point energies of the bremsstrahlung. Only a slight shift towards symmetry at higher excitation energies, due to the increase of the symmetric fission yield, is observed. On the contrary, the values for $^{240}\text{Pu}(\text{s.f.})$ are shifted about one mass unit towards symmetry compared to $^{239}\text{Pu}(n_{\text{th}},f)$. The average preneutron mass of the light and heavy fragment peaks, $\langle m_L^* \rangle$ and $\langle m_H^* \rangle$, calculated as mentioned in Sec. III B, show completely the same behavior as the average provisional masses $\langle \mu_L \rangle$ and $\langle \mu_H \rangle$. The $\langle m_L^* \rangle$ and $\langle m_H^* \rangle$ values for $^{239}\text{Pu}(n_{\text{th}},f)$ are in perfect agreement with the results of Neiler *et al.*,¹⁴ who obtained the values 100.34 and 139.66 u, respectively. Our results for the spontaneous fission of ^{240}Pu agree also within the uncertainties with the values $\langle m_L^* \rangle = 101.55 \pm 0.14$ u and $\langle m_H^* \rangle = 138.45 \pm 0.14$ u determined by Deruytter and Wegener-Penning.² These authors also observed the shift of the average light and heavy fragment mass towards symmetry for $^{240}\text{Pu}(\text{s.f.})$ compared to $^{239}\text{Pu}(n_{\text{th}},f)$. This is in disagreement with the results of Wagemans *et*

*al.*²² who found no difference between the $\langle m_L^* \rangle$ and $\langle m_H^* \rangle$ values for $^{239}\text{Pu}(n_{\text{th}},f)$ and $^{240}\text{Pu}(s.f.)$. In the $^{239}\text{Pu}(d,pf)$ reaction the average light and heavy fragment mass was also found to be constant above the resonance at 4.65 MeV ($\langle m_L^* \rangle = 100.3$ u and $\langle m_H^* \rangle = 139.7$ u; see Ref. 5). As can be seen from Table I, the width of the mass peaks $\sigma_{\mu_L} = \sigma_{\mu_H}$ increases with the excitation energy of the fissioning nucleus.

The provisional mass distributions for $^{240}\text{Pu}(s.f.)$, $^{239}\text{Pu}(n_{\text{th}},f)$, and the photofission of ^{240}Pu with 20-MeV bremsstrahlung are presented in Fig. 7. In the mass distribution for $^{240}\text{Pu}(s.f.)$ a prominent shoulder around mass 142 and complementary mass is present. The mass distribution has also a very high peak yield (more than 7%) around mass 134. These structures were also observed in the work of Toraskar and Melkonian.¹ They have practically disappeared in $^{239}\text{Pu}(n_{\text{th}},f)$ and already completely in the photofission of ^{240}Pu with 12-MeV bremsstrahlung. The largest differences between the mass distributions of

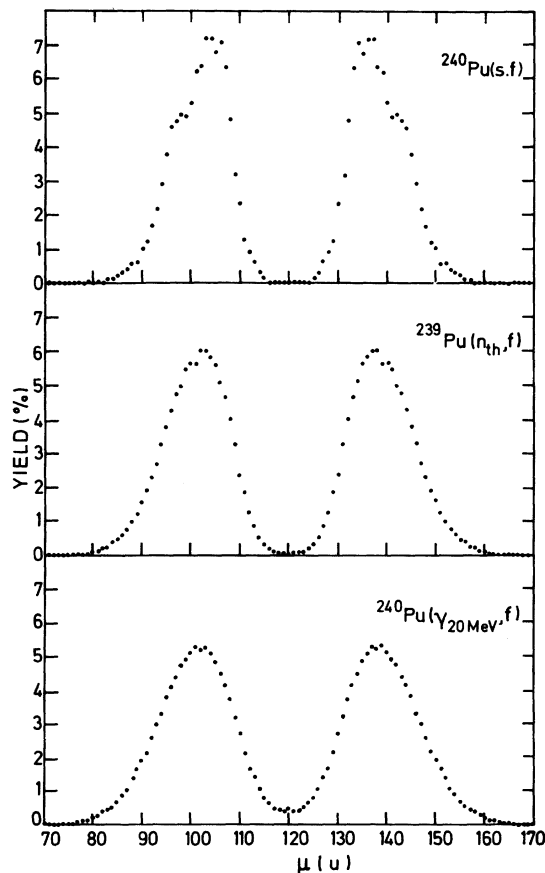


FIG. 7. Provisional mass distribution for $^{240}\text{Pu}(s.f.)$, $^{239}\text{Pu}(n_{\text{th}},f)$ and the photofission of ^{240}Pu with 20-MeV bremsstrahlung.

$^{240}\text{Pu}(s.f.)$ and $^{239}\text{Pu}(n_{\text{th}},f)$ appear in the mass region 133–134, where the mass distribution is strongly influenced by the spherical $N=82$ neutron shell. As could be seen on Fig. 2, the difference in the kinetic energy distribution of the fragments in the mass region 130–135 between $^{240}\text{Pu}(s.f.)$ and $^{239}\text{Pu}(n_{\text{th}},f)$ is only caused by fission events with high kinetic energy. So the high yield around mass 134 can be attributed to an enhanced production of the shell-stabilized scission configuration with low deformation in the mass region around the $N=82$ shell in $^{240}\text{Pu}(s.f.)$, compared to $^{239}\text{Pu}(n_{\text{th}},f)$. The shoulder in the mass distribution around mass 142 can be attributed to the strong shell correction for the deformed $N=88$ neutron shell. The disappearance of these shell effects in the mass distribution for $^{239}\text{Pu}(n_{\text{th}},f)$ can easily be understood, in the model of Wilkins *et al.*,⁹ by a slight increase of the intrinsic temperature in this case. These authors showed that for the fissioning system ^{236}U the structure in the mass distribution decreases rapidly, increasing the intrinsic temperature from 0.75 to 0.85 MeV. The observed shift towards asymmetry of the average light and heavy fragment mass in $^{239}\text{Pu}(n_{\text{th}},f)$ compared to $^{240}\text{Pu}(s.f.)$ is, at least for a large part, due to the decrease of the strong influence of the $N=82$ neutron shell.

IV. CONCLUSIONS

From our experiments we determined that the $\langle E_h^* \rangle$ value in $^{240}\text{Pu}(s.f.)$ is 1.2 ± 0.5 MeV higher than for $^{239}\text{Pu}(n_{\text{th}},f)$. In view of this result, the hypothesis of a superfluid fission mode below the fission barrier in the fissioning system ^{240}Pu , as proposed by Lachkar *et al.*,⁵ is questionable.

From the excitation energy dependence of $\langle E_h^* \rangle$ in the photofission of ^{240}Pu , a slope $d\langle E_h^* \rangle / d\langle E_{\text{exc}}(E_e) \rangle = -0.37 \pm 0.08$ is deduced. This value is in very good agreement with the values of $d\langle E_h^* \rangle / dE_{\text{exc}}$, reported in the literature for the compound system ^{240}Pu , produced in other reactions with small angular momentum transfer. The dependence of $E_h^*(m^*)$ on the excitation energy of the compound system shows that the observed changes in the kinetic energy release in photofission are due to the diminution of shell corrections at higher intrinsic temperatures, in agreement with the scission point model of Wilkins *et al.*⁹ The behavior of $\langle E_h^* \rangle(m^*)$ in our experiments shows also that, as generally observed, the fission degree of freedom is very weakly coupled to quasiparticle excitations.

Structures in the overall kinetic energy and provisional mass distributions, which can be attributed to the strong influence of the spherical $N=82$ neutron shell and the deformed $N=88$ neu-

tron shell are present for $^{240}\text{Pu}(s.f.)$. These structures have already practically disappeared in $^{239}\text{Pu}(n_{th},f)$, which is explained in the framework of the model of Wilkins *et al.*⁹ by the increase of the intrinsic temperature.

ACKNOWLEDGMENTS

This research was supported by the Interuniversitair Instituut voor Kernwetenschappen—Na-

tionaal Fonds voor Wetenschappelijk Onderzoek. Thanks are expressed to the linac team of our laboratory for the operation of the accelerator and to Dr. R. Van de Vijver and E. Kerkhove for their aid during the cross section measurements. The authors are also indebted to Dr. M. Nève de Mevergnies and Dr. C. Wagemans for their help during the measurements at the SCK-CEN Mol.

- ¹J. Toraskar and E. Melkonian, *Phys. Rev. C* **4**, 1391 (1971).
- ²A. J. Deruytter and G. Wegener-Penning, in *Proceedings of the Third International Symposium on the Physics and Chemistry of Fission, Rochester, 1973* (IAEA, Vienna, 1974), Vol. II, p. 51.
- ³J. Weber, H. J. Specht, E. Konecny, and D. Heunemann, *Nucl. Phys. A* **221**, 414 (1974).
- ⁴N. I. Akimov, V. G. Vorob'eva, N. N. Kabenin, N. P. Kolosov, B. D. Kuz'minov, A. I. Sergachev, L. D. Smirenkina, and M. Z. Tarosko, *Yad. Fiz.* **13**, 484 (1971) [*Sov. J. Nucl. Phys.* **13**, 272 (1971)].
- ⁵J. Lachkar, Y. Patin, and J. Sigaud, *J. Phys. Lett.* **36**, 79 (1975).
- ⁶B. B. Back, J. M. Lebowitz, and K. L. Wolf, *Phys. Rev. C* **20**, 1819 (1979).
- ⁷W. J. Swiatecki and S. Bjørnholm, *Phys. Rev. C* **4**, 325 (1972).
- ⁸D. M. Crawford, R. Koch, and H. H. Thies, *Nucl. Instrum. Methods* **109**, 573 (1973).
- ⁹B. D. Wilkins, E. P. Steinberg, and R. R. Chasman, *Phys. Rev. C* **14**, 1832 (1976).
- ¹⁰H. Nifenecker, J. Blachot, J. P. Bocquet, R. Brissot, J. Crançon, C. Hamelin, G. Mariolopoulos, and Ch. Ristori, in *Proceedings of the Fourth International Symposium on the Physics and Chemistry of Fission, Jülich, 1979* (IAEA, Vienna, 1980), Vol. II, p. 35.
- ¹¹J. S. Pruitt and S. R. Domen, NBS monograph 48, 1962.
- ¹²A. De Clercq, E. Jacobs, D. De Frenne, H. Thierens, P. D'hondt, and A. J. Deruytter, *Phys. Rev. C* **13**, 1536 (1976).
- ¹³H. W. Schmitt, W. E. Kicker, and C. E. Williams, *Phys. Rev.* **137**, B837 (1965).
- ¹⁴J. Neiler, F. Walter, and H. Schmitt, *Phys. Rev.* **149**, 894 (1966).
- ¹⁵N. S. Rabotnov, G. N. Smirenkin, A. S. Soldatov, L. N. Usachev, S. P. Kapitza, and Yu. M. Tsipenyuk, *Yad. Fiz.* **11**, 508 (1970) [*Sov. J. Nucl. Phys.* **11**, 285 (1970)].
- ¹⁶J. T. Caldwell, E. J. Dowdy, B. L. Berman, R. A. Alvarez, and P. Meyer, *Phys. Rev. C* **21**, 1215 (1980).
- ¹⁷L. Katz, T. M. Kavanagh, A. G. W. Cameron, E. C. Bailey, and J. W. T. Spinks, *Phys. Rev.* **99**, 98 (1955).
- ¹⁸R. Vandenbosch and J. R. Huizenga, in *Nuclear Fission* (Academic, New York, 1973).
- ¹⁹E. Jacobs, A. De Clercq, H. Thierens, D. De Frenne, P. D'hondt, P. De Gelder, and A. J. Deruytter, *Phys. Rev. C* **20**, 2249 (1979).
- ²⁰F. Manero and V. Koshin, *At. Energy Rev.* **10**, 637 (1972).
- ²¹M. Soleilhac, J. Frehaut, J. Gauriau, and G. Mosinski, in *Proceedings of the Second International Atomic Energy Conference on Nuclear Data for Reactors, Helsinki, Finland, 1970* (IAEA, Vienna, 1970), Vol. II, p. 145.
- ²²C. Wagemans, G. Wegener-Penning, H. Weigmann, and R. Barthelémy, in *Proceedings of the Fourth International Symposium on the Physics and Chemistry of Fission, Jülich, 1979* (IAEA, Vienna, 1980), Vol. II, p. 143.
- ²³N. P. Dyatchenko, V. N. Kabenin, N. P. Kolosov, B. D. Kuzminov, and I. Sergatchev, Institute of Physics and Energetics, Obninsk, USSR, Report No. 366, 1973.
- ²⁴Y. Patin, J. Lachkar, and J. Sigaud, National Soviet Conference on Neutron Physics, Kiev, 1975 (unpublished).
- ²⁵M. J. James, *J. Nucl. Energy* **23**, 517 (1969).
- ²⁶H. Nifenecker, C. Signarbieux, R. Babinet, and J. Poitou, in *Proceedings of the Third International Symposium on the Physics and Chemistry of Fission, Rochester, 1973* (IAEA, Vienna, 1974), Vol. II, p. 117.
- ²⁷J. Lachkar, J. Sigaud, Y. Patin, J. Chardine, and C. Humeau, Saclay Report No. CEA-R 4715, 1975.
- ²⁸J. C. D. Milton and J. S. Fraser, *Annu. Rev. Nucl. Sci.* **16**, 894 (1966).
- ²⁹J. P. Unik, J. E. Gindler, L. E. Glendenin, K. J. Flynn, A. Gorski, and R. K. Sjoblom, in *Proceedings of the Third International Symposium on the Physics and Chemistry of Fission, Rochester, 1973* (IAEA, Vienna, 1974), Vol. II, p. 19.
- ³⁰P. David, J. Debrus, J. Schulze, H. N. Harakeh, H. v. d. Plicht, and A. van der Woude, in *Proceedings of the Fourth International Symposium on the Physics and Chemistry of Fission, Jülich, 1979* (IAEA, Vienna, 1980), Vol. I, p. 373.
- ³¹M. Asghar, F. Caitucoli, P. Perrin, and C. Wagemans, *Nucl. Phys. A* **311**, 205 (1978).
- ³²K. L. Wolf, W. Loveland, and C. T. Roche (unpublished).